Molecular-beam epitaxy of AlInN: An effect of source flux and temperature on indium atom incorporation in alloys

Z. Y. Wang,[1] B. M. Shi,[1] Y. Cai,[2] N. Wang,[2] and M. H. Xie[1]
[1]*Department of Physics, The University of Hong Kong, Pokfulam Road, Hong Kong*
[2]*Department of Physics, Hong Kong University of Science and Technology, Clear Water Bay, Kowloon, Hong Kong*

(Received 29 December 2009; accepted 21 May 2010; published online 3 August 2010)

Growth of AlInN alloys by molecular-beam epitaxy is studied by reflection high-energy electron diffraction, where in-plane lattice constant and specular beam intensity oscillations are recorded for information of lattice misfit and growth rate as a function of source flux and temperature. An unexpected dependence of alloy growth rate on indium flux is observed, which reflects the specific incorporation kinetics of indium in the alloy. © *2010 American Institute of Physics*.
[doi:10.1063/1.3456009]

I. INTRODUCTION

The alloy of $Al_{1-x}In_xN$ $(0 \leq x \leq 1)$ has attracted considerable attention in the past decade due to its promise in optoelectronic and photovoltaic applications.[1–9] Alloys of different compositions may be epitaxially grown on GaN, a close cousin of AlInN that has matured into wide commercial availability. The lattice misfit strain between GaN and $Al_{1-x}In_xN$ can be tensile or compressive, depending on the composition x of the alloy. One may thus fabricate strain-compensated heterostructures on GaN by stacking layers of $Al_{1-x}In_xN$ with different compositions. Moreover, as the alloy of $Al_{0.82}In_{0.18}N$ has the same lattice constant as GaN, one can grow multilayers of $Al_{0.82}In_{0.18}N/GaN$ without introducing strain-relieving defects. Such multilayered structures can be used as the Bragg mirrors in vertical-cavity surface emitting lasers, for example.[2,3]

Although there have been a number of reports on the growth of $Al_{1-x}In_xN$ using techniques such as molecular-beam epitaxy (MBE) (Refs. 6–9) and metal-organic vapor phase epitaxy,[2–5] it remains problematic to obtain high quality alloy films with arbitrary compositions. Alloys with intermediate compositions tend to phase-separate, leading to heterogeneous films rather than homogeneous alloy layers.[10–13] To overcome such a problem, one may resort to techniques that operate at far-from-equilibrium, such as MBE, so phase-separation may be suppressed by kinetics. However, even for MBE growth of the alloy, complications remain, one of which is the complex incorporation kinetics of the constituent atoms at the surface.[9]

In a previous experiment, we used reflection high-energy electron diffraction (RHEED) to follow the epitaxial growth mode and incorporation behavior of the cation atoms (Al and In) at a low temperature.[9] Here, we extend the previous study to a wider range of temperature and flux. The RHEED technique is again used for evaluation of alloy growth mode, deposition rate and strain of the epitaxial films. *Ex situ* secondary ion mass spectrometry (SIMS) and transmission electron microscopy (TEM) are also conducted for some samples, supplementing the RHEED studies *in situ*. It is observed that incorporation of indium atoms shows a complex temperature and flux dependence, which is incomplete despite the relatively low temperatures adopted for the alloy deposition.

II. EXPERIMENT

The MBE system was equipped with conventional effusion cells of Ga, Al, and In sources and a radio-frequency plasma unit for nitrogen (N). The RHEED was operated at 10 KeV and the diffraction pattern and its specular beam intensity oscillations were recorded using a charge-coupled device camera interfaced to a computer. The substrates were GaN-on-SiC(0001) from TDI Inc., on which GaN buffer films were first grown under the Ga-stable condition.[14] The resulted Ga-polar GaN buffer-films were then treated by N-plasma at 600 °C till the (2×2) reconstruction appeared, after which, deposition of $Al_{1-x}In_xN$ were carried out at temperatures between 350 and 600 °C. For alloy depositions, a fixed flux of nitrogen at $F_N \sim 1.1\times10^{14}$ atoms/cm^2 s (corresponding to a growth rate of ~0.05 bilayers/second (BLs/s), where 1 BL$=c/2$, with c being the lattice constant along [0001], the growth direction of III-Nitrides) and of Al at $F_{Al} \sim 1.1\times10^{13}$ atoms/cm^2 s (corresponding to a growth rate of ~0.005 BLs/s) were used, while the flux of In was varied from 1.65×10^{11} to 5.5×10^{13} atoms/cm^2 s (the corresponding In-to-Al flux ratio changed from 0.15 to 5.0). All the source fluxes were calibrated by the RHEED intensity oscillations during AlN, GaN, and InN growth and by thickness measurements of the grown films.[9,14] Sample heating were achieved by flowing direct currents through the long sides of the rectangular sample pieces (size: 11×4 mm^2) and the temperatures were measured by a Raytek infrared pyrometer. The lowest temperature experimented here was achieved by switching off the heating current and its value was beyond the measurable range of the pyrometer. However, due to the heat radiation from the high-temperature source cells, the surface temperature of the sample could still be high. From a linear extrapolation of the temperature versus heating-power dependence, we estimated it to be close to 350 °C. For some of the thick films grown, SIMS and TEM experiments were carried out using a time-of-flight second-

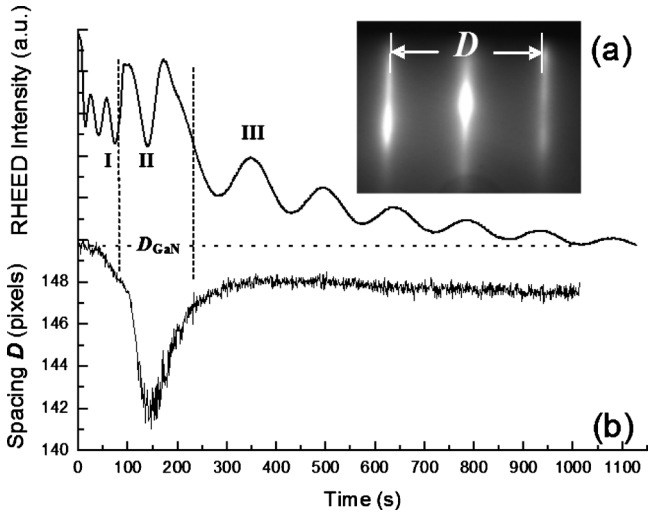

FIG. 1. (a) The RHEED intensity oscillations during AlInN deposition at 430 °C, using an In-to-Al flux ratio of ~3.3. Note the different growth stages (I–III) as separated by the dashed lines. The inset shows the RHEED pattern taken from the alloy surface along $[11\bar{2}0]$, and the marked "*D*" measures the spacing between the (01) and $(0\bar{1})$ diffraction streaks. (b) Evolution of *D* during alloy deposition, and the horizontal dotted line marks the measured value of *D* from GaN substrate.

ary ion mass spectrometer ToF-SIMS V (ION-TOF GmbH) and a Joel TEM2010F microscope, respectively. For the former, oxygen sputtering ion was used, while for cross-sectional TEM sample preparation, the standard procedure of mechanical polishing followed by Ar-ion milling was followed.

III. RESULTS AND DISCUSSIONS

A. Lattice misfit and the RHEED intensity oscillations

To grow $Al_{1-x}In_xN$ alloys with different compositions, we varied the flux of In while maintaining the fluxes of Al and N constant as mentioned earlier. The total flux of metals, i.e., $F_{In}+F_{Al}$, was kept below that of nitrogen (F_N), so the growth was under the excess-N regime. In this growth regime, film growth rate was dependent on the flux of metals but independent on F_N, as confirmed by our RHEED oscillation experiments.

Figure 1(a) shows an example of the RHEED specular beam intensity oscillations, where the inset shows the corresponding diffraction pattern along $[11\bar{2}0]$. Figure 1(b) presents, on the other hand, an evolution of the measured reciprocal lattice parameter $D \propto 1/a$, where *a* is the in-plane lattice constant [refer to Fig. 1(a) inset].

Both the streaky RHEED pattern and the persistent intensity oscillations [Fig. 1(a)] suggest a two-dimensional (2D) layer-by-layer growth mode of the alloy on GaN. However, transition of the streaky pattern into a spotty one was occasionally observed following prolonged deposition. Such transitions were gradual, which pointed to a kinetic roughening process rather than a growth mode change. It was also observed from the RHEED patterns that the grown alloys were usually tilted with respect to the substrate surface [see Fig. 1(a) inset] and the largest angle of tilting was recorded to be ~6°.

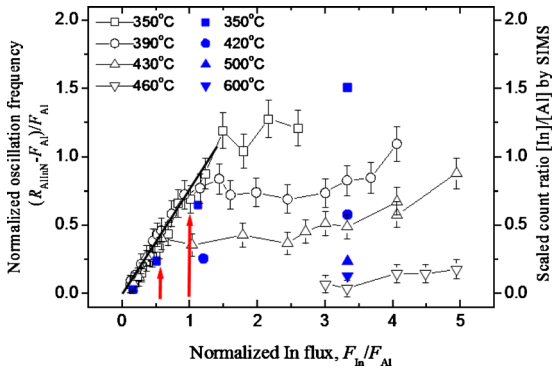

FIG. 2. (Color online) Normalized In incorporation rate (open symbols), as measured by the RHEED intensity oscillations in the stable growth stage, as a function of (normalized) In flux. Different symbols refer to different growth temperatures. The scaled count ratio between In and Al obtained by SIMS measurements are shown by solid symbols for comparison. The dark solid line has a slope of 0.77, and the two vertical arrows mark the critical flux F_c at which the rates become saturated for deposition at $T=390$ and 430 °C.

From Fig. 1, one also observes complications in the oscillation frequency and the lattice parameter evolution. Specifically, three deposition stages may be identified, where in the very early stage I, the RHEED intensity undergoes a rapid oscillation for a couple of periods, followed by a transient stage II before stabilizing in the final oscillation stage III. Correspondingly in Fig. 1(b), one observes a change in lattice constant: upon the commencement of deposition, *D* starts to deviate from that of GaN (D_{GaN}), implying an initiation of AlInN alloy growth. It reaches an extreme value in stage II and then recovers and stabilizes in stage III at values dependent on source flux and temperature. Such a transient growth behavior suggests a change in the structure and/or composition of the surface due to some specific kinetic processes in the early stage of deposition.

It has been known for long that persistent RHEED intensity oscillations reflect the 2D growth of a film, and the period of the oscillation corresponds to the time of one atomic monolayer (ML) or BL growth of the epifilm.[15] The RHEED oscillations thus provide a direct and convenient measure of epitaxial growth rate.[14,15] In stage I and II of AlInN growth, however, we found no obvious correlation between the oscillation frequency and source flux. For example, in stage I, a roughly constant rate of ~0.03 s^{-1} was measured, while in stage II, the oscillation frequency was not constant. Therefore, it is not certain if these oscillations reflect the epitaxial growth rates. Additionally, we noted a structural and morphological change in the surface upon the commencement of alloy deposition, where the initial rougher and (2×2) structured substrate surface changed to one showing a smoother morphology but the (1×1) structure. Such a change would have contributed partly to the intensity variations in the RHEED.

For the stable oscillation stage III, a flux dependence of the oscillation frequency was indeed observed. Figure 2 summaries such dependences at different growth temperatures. In the figure, instead of plotting the oscillation frequency R_{AlInN}, the rate due to incorporation of In, R_{InN}, measured with respect to the flux of Al, are plotted as a function of In

flux. The latter has also been normalized by F_{Al}. Due to the fact that Al incorporation is complete, or $R_{AlN}=F_{Al}$, as established previously in Ref. 9 and confirmed during the course of this investigation, we deduce that the incorporation rate of In is $R_{InN}/F_{Al}=(R_{AlInN}-R_{AlN})/F_{Al}=(R_{AlInN}-F_{Al})/F_{Al}$. Obviously, this quantity $(R_{InN}/F_{Al}=R_{InN}/R_{AlN})$ also reflects the ratio between In and Al contents in the alloy, $x/(1-x)$. Therefore, for comparison, the measured count ratio [In]/[Al] by SIMS are also presented in the figure. Note, however, that the SIMS data have been scaled by a relative sensitivity factor (RSF) of 0.3, which is chosen simply to make the data being consistent with the RHEED results (refer to Fig. 5 below). As is shown, for growth at low In fluxes, an approximately linear dependence of R_{InN} on F_{In} is observed. At intermediate fluxes, however, deviation from the linear dependence is apparent. Changing the flux no longer changes the rate R_{InN}. Instead, the rate seems to saturate at a value dependent on temperature only. The higher the temperature, the lower the saturated rate. At even higher fluxes, a reentrant but weak dependence between R_{InN} and F_{In} becomes discernable. Such a behavior suggest a complex incorporation kinetics of In during AlInN growth by MBE.

B. Indium incorporation kinetics

In the following, we consider the incorporation behavior of indium in more detail. As mentioned earlier, in the excess-N growth regime of MBE, alloy growth rate is independent on F_N, but depends on the fluxes of Al and In. So we may write

$$R_{AlInN}=R_{InN}+R_{AlN}=\alpha_{In}F_{In}+\alpha_{Al}F_{Al}, \quad (1)$$

where α_{In} and α_{Al} are the incorporation coefficients of In and Al, respectively. Experiments have shown that Al incorporation is complete,[9] i.e., $\alpha_{Al}=1$, so the above expression can be rearranged into

$$\frac{R_{AlInN}-F_{Al}}{F_{Al}}=\frac{R_{InN}}{F_{Al}}=\alpha_{In}\frac{F_{In}}{F_{Al}}, \quad (2)$$

a quantity that is plotted in Fig. 2. A linear dependence between R_{InN}/F_{Al} and F_{In}/F_{Al} is thus expected if α_{In} is a constant. This is indeed the case in the low flux region of Fig. 2, and a least-square fitting of the data gives rise to a value of $\alpha_{In}\approx 0.77$ (solid line in figure), agreeing with the result of Ref. 9. Moreover, from Fig. 2, one notes the slope of the linear dependence or α_{In} does not seem to be sensitive to temperature.

First, the result of $\alpha_{In}<1$ suggests an incomplete incorporation of indium from the flux, which is unexpected at the low temperature of this experiment. Indeed, surface desorption of atoms from the surface cannot be significant at such temperatures. If not desorbed, the unincorporated In atoms would remain on surface. To show this, we performed an Auger electron spectroscopy (AES) measurement of a sample immediately after the growth experiment. The spectrum (not shown) did reveal In signals. Furthermore, the SIMS measurement of a film showed a high concentration In (and Ga) near the surface region (Fig. 3). In fact, metallic droplets were often observed on surface following some

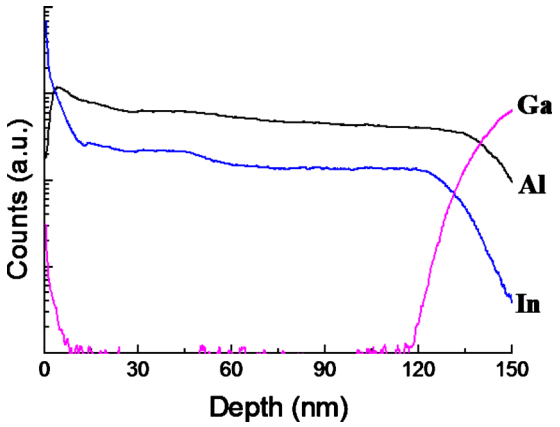

FIG. 3. (Color online) SIMS depth profile of In, Al, and Ga contents in an alloy (growth condition: $T=420$ °C, $F_{In}/F_{Al}\sim 1.2$).

thick film depositions. Therefore, we affirm that incomplete In incorporation has led to an accumulation of excess metal on surface, possibly in the form of droplets. In some previous studies of GaN growth by MBE, Ga adlayers were seen to wet the surface when an excess Ga flux (i.e., $F_{Ga}/F_N>1$) was used.[16–18] Although we cannot rule out the possibility of a similar wetting layer on the surface of AlInN, where the condition of $F_{Al+In}/F_N<1$ was used instead, the presence of such a wetting layer would appear less reconcilable with the fact that the growth rate depends on the flux of metals but is independence on N flux. As such, in our later analysis in section III(D), we shall assume the unincorporated In are simply trapped in droplets, which are growth inactive.

When the source flux is above a critical value, the RHEED intensity oscillations show a saturated frequency, implying a constant rate of indium incorporation, irrespective of the supply of atoms from the flux. In such a growth regime, however, increasing the temperature reduces the saturated rate of incorporation.

Evidence of reduced In incorporation (and unchanged Al incorporation) with temperature is also found from the SIMS measurement of a sample as shown in Fig. 4. The sample consists of three layers of AlInN sandwiched between GaN spacing layers as depicted in the inset of Fig. 4(a). A cross-sectional TEM micrograph of the sample is shown in Fig. 4(b). The three alloy layers were grown under the same flux condition (i.e., $F_{Al}\sim 2.3\times 10^{13}$ atoms/cm^2 s and $F_{In}\sim 7.6\times 10^{13}$ atoms/cm^2 s, which differ from those adopted in the RHEED experiment for a higher growth rate), while the growth temperatures were at 600, 500, and 420 °C for the bottom, middle, and top (close to surface) alloy layers, respectively. The descending order of the temperature variation was to minimize a possible decomposition or interlayer diffusion of atoms in the bottom layers during top layer growth. Prior to SIMS experiment, the sample was etched by HCl in order to remove excess metal from the surface. The SIMS depth profiles of In, Al, and Ga clearly shows a reduction in In content in the alloy with increasing temperature, while that of Al remains approximately constant.

Figure 5 summarizes, in an Arrhenius plot, the temperature dependence of In incorporation rates induced by the RHEED measurements as well as the measured count ratio

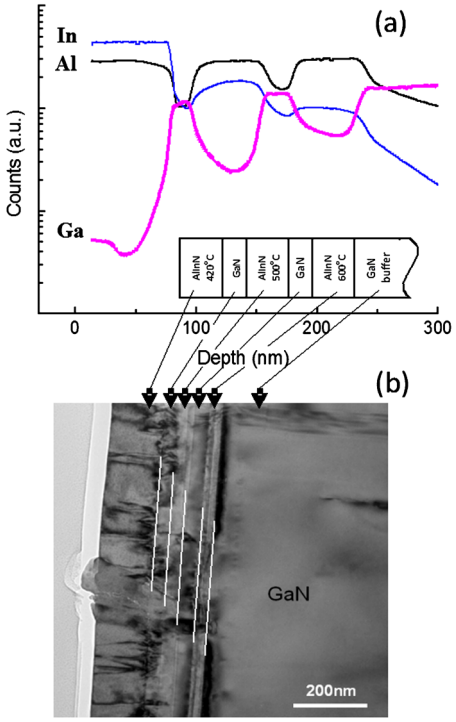

FIG. 4. (Color online) (a) SIMS depth profile of In, Al, and Ga contents in a layered sample grown at one and the same flux condition ($F_{In}/F_{Al} \sim 3.3$) but varying temperatures. The inset shows a schematic drawing of the sample structure and (b) shows a cross-sectional TEM micrograph of the sample. For the depth profiling, no correction of the sputtering rates in different layers has been taken into account.

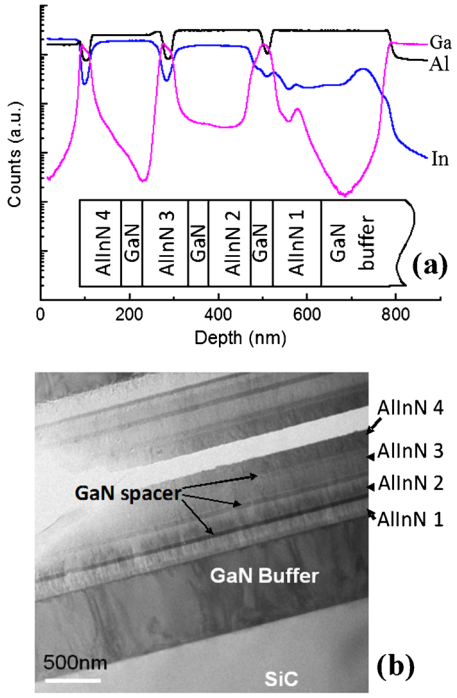

FIG. 6. (Color online) (a) SIMS depth profile of In, Al, and Ga contents in a layered sample grown at the constant temperature of $T \sim 350$ °C but changing In and Al fluxes. The corresponding flux ratios are 0.15, 0.51, 1.12, and 3.33 for AlInN layers 1, 2, 3, and 4, respectively. The inset shows a schematic drawing and (b) presents a cross-sectional TEM micrograph of the sample.

of [In]/[Al] by the SIMS. For the latter, scaling of the raw data by a RSF ~0.3 was shown to make them consistent with the RHEED results. Least-square fitting (solid line) gives rise to an energy of 0.45 ± 0.05 eV, which is well below the energy of desorption of atoms from surface (~1.9 eV).[19]

Finally, as the flux of In is increased further, the RHEED measurements show a reentrant dependence of the growth rate on In flux, though it is much weaker than that in the low flux region. Alloys with high In contents can thus be fabricated using high In-to-Al flux ratios. As an example, Fig. 6(a) shows the SIMS measurement of a sample grown at a constant temperature of ~350 °C but varying In and Al fluxes for different alloy layers. To ensure a similar growth rate for the different layers, the total flux of metals, $F_{Al} + F_{In}$, was made approximately constant. The schematic diagram of the sample is shown in the inset while a cross-sectional TEM micrograph of the sample is shown in Fig. 6(b).

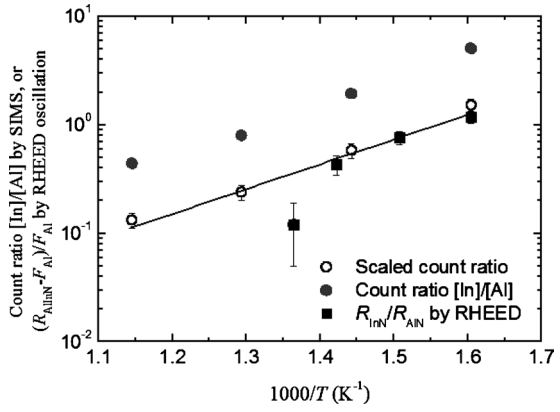

FIG. 5. Arrhenius plot of the saturated growth rates in the intermediate flux range of the deposition. Data from the SIMS (Fig. 4) are also included for comparison. The line represents an Arrhenius fitting of the data, giving rise to an energy of 0.45 ± 0.05 eV.

It is noted in passing from the TEM micrograph that the contrast of the GaN spacing layer appears lighter for the top, closer to surface layer than that of the bottom one. This indicates an increasing amount of In being incorporated in GaN as the growth proceeded. It suggests again the presence of excess In on the growing front, some of which are inevitably incorporated during GaN layer deposition.

C. Lattice constant and strain

In addition to the RHEED oscillations, diffraction patterns from the grown alloys were also recorded as exemplified in the inset of Fig. 1(a). Particularly, the spacing D between the (01) and $(0\bar{1})$ diffraction streaks was measured as a function of deposition time (film thickness), which has been shown in Fig. 1(b). By comparing to D_{GaN}, the spacing measured from GaN substrate, in-plane lattice constants of the grown alloys are derived.

Consistent with the RHEED oscillation data, the initial stage deposition shows a transient behavior in the measured D. Specifically, from Fig. 1(b), one observes that the initial deposit shows alloys with changing In content (thus a changing lattice constant and D). In the stable growth stage III, on

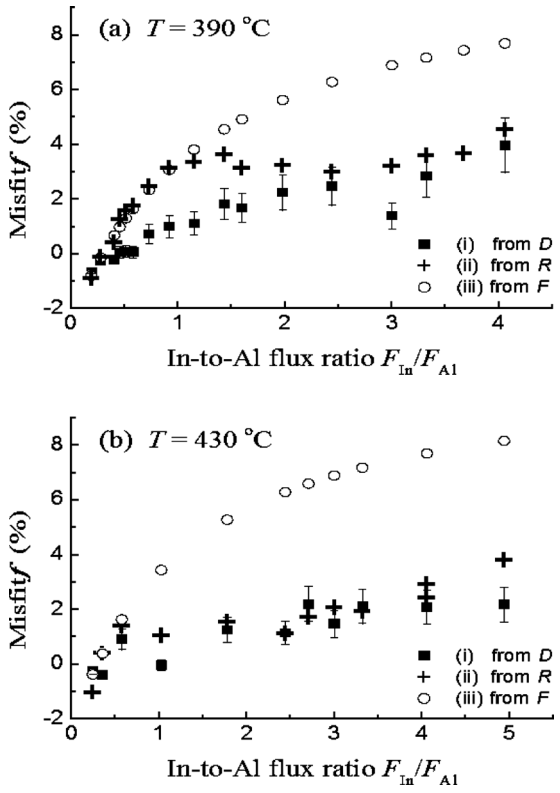

FIG. 7. Lattice misfit f between AlInN and GaN derived from (i) lattice constant measurement by the RHEED, (ii) growth rate measurement by the RHEED intensity oscillations, and (iii) calculated from the flux, assuming constant incorporation coefficients, $\alpha_{In}=0.77$ and $\alpha_{Al}=1$. (a) is for growth at 390 °C and (b) at 430 °C.

the other hand, an alloy with a constant lattice parameter and thus a constant composition is produced. Figures 7(a) and 7(b) plot the lattice misfit, f, derived from the measured D after 5–10 periods of the RHEED oscillations in the stable growth stage III. The f is calculated from D according to

$$f = (a^{\parallel}_{\mathrm{AlInN}} - a^{\parallel}_{\mathrm{GaN}})/a^{\parallel}_{\mathrm{GaN}} = (D_{\mathrm{GaN}} - D)/D, \tag{3}$$

where $a^{\parallel}_{\mathrm{AlInN}}$ and $a^{\parallel}_{\mathrm{GaN}}=a_{\mathrm{GaN}}$ are in-plane lattice constants of the grown alloy and GaN substrate, respectively, and a_{GaN} refers to the lattice constant of a strain-free GaN. Figure 7(a) is for growth at 390 °C and Fig. 7(b) is for growth at 430 °C. Since the measured D's were for ultrathin epilayers, the data in Figs. 7(a) and 7(b) may not reflect theoretical lattice misfits of the grown alloys due to residual strains in the epilayer. The "theoretical" misfit $f_0=(a_{\mathrm{AlInN}}-a_{\mathrm{GaN}})/a_{\mathrm{GaN}}$, where a_{AlInN} is the lattice constant of a strain-free alloy, may be estimated from the growth rates using Eq. (2), corresponding to $x/(1-x)$, and using the Vegard's law to calculate the lattice constant of the alloy with composition x: $a_{\mathrm{AlInN}}=(1-x)a_{\mathrm{AlN}}+xa_{\mathrm{InN}}$. Such results are also plotted in Fig. 7. Further, if we take the incorporation coefficients for In and Al constant at $\alpha_{In}=0.77$ and $\alpha_{Al}=1$ throughout the whole flux range, the grown alloys would have compositions given by $x=\alpha_{In}F_{In}/(\alpha_{In}F_{In}+F_{Al})$, from which a new set of data of f may be derived, as shown in the figure by the open circles.

As is seen, a general agreement is achieved between data from the lattice spacing D measurement (solid squares) and from those of the RHEED oscillations (crosses), especially for high In fluxes. Both sets of data differ by a large margin from those estimated from the flux. This is not surprising, as In incorporation coefficient is *not* constant as already discussed early in Sec. III B. On the other hand, constant $\alpha_{In}=0.77$ and $\alpha_{Al}=1$ are indeed valid for low fluxes and the calculated misfits based on flux and growth rate expectedly agree with each other, as is shown in Fig. 7. However, in such a low flux region, lattice misfits derived from the D measurements deviate from the above two, particularly in Fig. 7(a). Although we are uncertain about the source of such deviations, one possibility is related to the residual strain in the thin epilayer. For alloys grown at low In fluxes, the content of indium is low and so, for the given thin epilayer, the misfit strain may not be fully relaxed. The in-plane lattice constant of the alloy takes a value closer to that of GaN substrate, leading to smaller f than that of a strain-free alloy (f_0). At high In fluxes, on the other hand, the resulted alloys have high In contents and even for the thin epilayer, the lattice misfit strain may have completely relaxed[20] and the agreement between f and f_0 is better. Another possibility is that the lattice constant measurement by the RHEED is for surface layer only, which may not have the same composition as in the bulk. An additional source of error can be related to the validity of the Vegard's law in calculating the lattice constant (and misfit) from x. As a result, a perfect agreement between the various data cannot be expected.

D. Discussion

In the following, we provide a further discussion on the incorporation kinetics of indium during AlInN growth by MBE. There are two separate issues: (1) the transient growth in the initial stage of deposition and (2) the complex dependence of indium incorporation rate on flux and temperature.

As suggested from the result of Fig. 2, at least a proportion of 23% of In from the flux does not contribute to the alloy growth. Neglecting the effect of desorption, such unincorporated In would accumulate on surface as confirmed by SIMS (Fig. 3) and AES measurements. An immediate consequence of this will be a surface with an excess In stoichiometry over that dictated by flux. Indeed, after only a few layers of film deposition, the surface would have contained so much excess indium that the growth would become in a metal-stable regime instead of excess-N. It is then quite puzzling why the growth rate remains being dependent on the flux of metals but independent on N flux. We attribute this to the possibility that the excess In on surface are not "growth-active" but are trapped in a reservoir of In-droplets on surface. These droplets grow in volume by atom aggregation, consuming some of the surface atoms and leaving a decreased amount to be incorporated in alloy films.

Ignoring desorption of atoms from surface, the change in In surface coverage (θ_s) of the "growth-active" indium is:[5]

$$\frac{d\theta_s}{dt} = F - k_I\theta_s - k_T\theta_s, \tag{4}$$

where F is the flux, k_I and k_T are the rate-constants of atom incorporation in film and surface-trapping in droplets, re-

spectively. Here, only the first-order kinetics is considered for simplicity. Obviously, the term $k_I\theta_s$ gives rise to the incorporation rate R_{InN} introduced earlier in Eq. (1), i.e.,

$$R_{InN} = k_I\theta_s = \alpha_{In}F_{In}. \quad (5)$$

Integrating Eq. (4), one gets

$$\theta_s(t) = \left(\frac{F}{k_I + k_T}\right)[1 - e^{-(k_I+k_T)t}]. \quad (6)$$

If the rate constants k_I and k_T are not large, it will take a few layers of deposition before θ_s. can reach the steady state value of F/k_I+k_T. It is thus possible that the delayed realization of steady state surface coverage is partly responsible for the observed transient growth dynamics as seen by the RHEED. After the steady state is reached with the constant surface coverage $\theta_s=F/k_I+k_T$, the steady state growth rate (region III) will be $R_{InN}=k_I\theta_s=k_IF/k_I+k_T$ according to Eq. (5). A linear dependence between R_{InN} and F is thus expected and the proportional constant is $\alpha_{In}=k_I/k_I+k_T$. This is obviously less than unity if k_T is not negligible comparing to k_I. The experimentally derived value of $\alpha_{In}\approx 0.77$ in the low flux region of Fig. 2 implies $k_T/k_I\approx 0.30$. Given the temperature dependence of $k_I\propto\exp(E_I/k_BT)$ as shown in Fig. 5 (k_B is the Boltzmann constant) and assuming a similar T-dependence of k_T, the ratio of $k_T/k_I\approx 0.30$ translates into an energy difference between k_T and k_I of about $\Delta E \sim 0.07$ eV. Such a small value of ΔE may then explain the insensitiveness of α_{In} to temperature as shown in Fig. 2.

When the source flux is increased to above a critical value of $F_c\sim k_I+k_T$, the steady state surface coverage will reach a full layer ($\theta_s=1$ ML), after which the growth rate becomes saturated at $k_I\theta_s=k_I$, which would be independent on flux but dependent on temperature only. Although the atomic details of In atom incorporation is still unclear, from the results of Fig. 5 and the derived energy of 0.45 eV, it is likely dictated by diffusion or step-pyrolysis.[21,22] In this flux regime, increasing the flux will only contribute more to droplet formation and growth. Since k_I (and k_T) decreases with temperature (Figs. 2 and 5), so will be the critical flux F_c. For example, at $T=390$ °C, the saturated incorporation rate of In is seen to be $k_I\approx 0.76F_{Al}$ and so $k_T\approx 0.3k_I\approx 0.23F_{Al}$. Then $F_c=k_I+k_T\approx 0.99F_{Al}$. At $T=430$ °C, on the other hand, the data of Fig. 2 shows $k_I\approx 0.43F_{Al}$, and so $k_T\approx 0.13F_{Al}$. Thus $F_c\approx 0.56F_{Al}$. These estimations of F_c are in agreement with the experiments (refer to the arrows in Fig. 2).

At even higher fluxes, some other effects that have so far been neglected may become non-negligible, causing the observed reentrant increase in growth rate with flux. One of such effects is the dependence of k_I on composition x. For example, at low fluxes, the alloys contain low indium contents (x) in the matrix of AlN. The local strain as caused by the size difference between In and Al atoms may favorably displace the incorporated In back to the surface. On the other hand, for growth at high In fluxes, the resulted alloys have higher In concentration, and the local strain profiles may no longer favor In expulsion. A consequence will be an increased atom incorporation.

IV. SUMMARY

The RHEED intensity oscillations and lattice constant evolution during AlInN alloy growth by MBE are analyzed. A transient growth dynamics and a complex flux and temperature dependence of indium atom incorporation are noted, which is attributed to a surface trapping process of In atoms.

To achieve $Al_{1-x}In_xN$ alloys with high In contents, one may either tune In-to-Al flux ratio or using low deposition temperature. Because of the different dependences of growth rate and alloy content on flux and temperature in different growth regimes, a detailed calibration is necessary in order to achieve a better control of film thickness and alloy composition.

ACKNOWLEDGMENT

We acknowledge the technical support from Mr. W. K. Ho. This work was financially supported by grants from the Research Grant Council of the Hong Kong Special Administrative Region, China, under the Grant Nos. HKU 7055/06P and 7048/08P.

[1] A. Trampert, O. Brandt, and K. H. Ploog, in *Gallium Nitrides I, Semiconductor and Semimetals*, edited by J. I. Pankove and T. D. Moustakas (Academic, New York, 1998), Vol. 50, Chap. 7.
[2] J.-F. Carlin and M. Ilegems, Appl. Phys. Lett. **83**, 668 (2003).
[3] T. C. Sadler, M. J. Kappers, and R. A. Oliver, J. Cryst. Growth **311**, 3380 (2009).
[4] C. Hums, J. Bläsing, A. Dadgar, A. Diez, T. Hempel, J. Christen, A. Krost, K. Lorenz, and E. Alves, Appl. Phys. Lett. **90**, 022105 (2007).
[5] H. P. D. Schenk, M. Nemoz, M. Korytov, P. Vennéguès, A. D. Dräger, and A. Hangleiter, Appl. Phys. Lett. **93**, 081116 (2008).
[6] M. J. Lukitsch, Y. V. Danylyuk, V. M. Naik, C. Huang, G. W. Auner, L. Rimai, and R. Naik, Appl. Phys. Lett. **79**, 632 (2001).
[7] M. Higashiwaki and T. Matsui, J. Cryst. Growth **251**, 494 (2003).
[8] W. Terashima, S.-B. Che, Y. Ishitani, and A. Yoshikawa, Jpn. J. Appl. Phys., Part 2 **45**, L539 (2006).
[9] B. M. Shi, Z. Y. Wang, M. H. Xie, and H. S. Wu, Appl. Phys. Lett. **92**, 101902 (2008).
[10] T. Matsuoka, Appl. Phys. Lett. **71**, 105 (1997).
[11] J. Adhikari and D. A. Kofke, J. Appl. Phys. **95**, 6129 (2004).
[12] T. Takayama, M. Yuri, K. Itoh, T. Baba, and J. S. Harris, Jr., Jpn. J. Appl. Phys., Part 1 **39**, 5057 (2000).
[13] M. Ferhat and F. Bechstedt, Phys. Rev. B **65**, 075213 (2002).
[14] S. M. Seutter, M. H. Xie, W. K. Zhu, L. X. Zheng Huasheng Wu and S. Y. Tong, Surf. Sci. **445**, L71 (2000).
[15] J. H. Neave, B. A. Joyce, P. J. Dobson, and N. Norton, Appl. Phys. A: Mater. Sci. Process. **31**, 1 (1983).
[16] A. R. Smith, R. M. Feenstra, D. W. Greve, M.-S. Shin, M. Skowronski, J. Neugebauer, and J. E. Northrup, J. Vac. Sci. Technol. B **16**, 2242 (1998).
[17] J. E. Northrup, J. Neugebauer, R. M. Feenstra, and A. R. Smith, Phys. Rev. B **61**, 9932 (2000).
[18] H. Zheng, M. H. Xie, H. S. Wu, and Q. K. Xue, Phys. Rev. B **75**, 205310 (2007).
[19] E. Dimakis, E. Iliopoulos, K. Tsagaraki, Th. Kehagias, Ph. Komninou, and A. Georgakilas, J. Appl. Phys. **97**, 113520 (2005).
[20] J. W. Matthews and A. E. Blakeslee, J. Cryst. Growth **27**, 118 (1974).
[21] I. Stanley, G. Coleiny, and R. Venkat, J. Cryst. Growth **251**, 23 (2003).
[22] A. Robertson, Jr., T. H. Chiu, W. T. Tsang, and J. E. Cunningham, J. Appl. Phys. **64**, 877 (1988).